Cryo-Transmission Electron Microscopy Confirms Controlled Synthesis of Cadmium Sulfide Nanocrystals within Lecithin Vesicles

Michael T. Kennedy,[‡] Brian A. Korgel,[†] Harold G. Monbouquette,*[,†,§] and Joseph A. Zasadzinski*[,‡,||]

Chemical Engineering Department, 5531 Boelter Hall, Box 951592, University of California, Los Angeles, Los Angeles, California 90095-1592, and Chemical Engineering Department, 3355 Engineering II, University of California, Santa Barbara, Santa Barbara, California 93106-5080

Received November 13, 1997. Revised Manuscript Received May 25, 1998

Size-quantized CdS nanocrystals of controlled dimensions are synthesized within monodisperse egg lecithin vesicles made by detergent depletion. Cryo-transmission electron microscopy (cryo-TEM) enables imaging in situ both of the vesicle wall and of the encapsulated nanocrystal. Cryo-TEM images confirm that only one particle per vesicle forms and that nanocrystal diameter is determined by the number of Cd^{2+} ions initially encapsulated. These micrographs further show that the particles adsorb to the inner surface of the vesicle membrane, which suggests that crystal growth and particle core structure could be controlled through manipulation of vesicle bilayer chemistry.

Introduction

Living organisms accurately and routinely produce complex, spatially well-defined and functional, mesoscopic structures, often with the aid of specific noncovalent molecular interactions. This self-assembly approach to materials processing and chemical control, as optimized by organisms through years of evolution, may provide the technological insight needed for efficient production of nanoscale devices and new materials designed at the molecular level.[1,2] Using a strategy that mimics the controlled synthesis of magnetite particles by magnetobacteria,[3,4] we demonstrate that phospholipid vesicles can be used for the synthesis of size-quantized CdS nanocrystals of predictable and controllable size.

Size-quantized semiconductor nanocrystals or "quantum dots" represent an exciting new class of materials that exhibit essentially bulk crystalline structure, yet their electronic properties lie between bulklike and molecular.[5−9] Quantum confinement of electrons within these nanoscale semiconductor particles leads to nanocrystal size-dependent electronic properties that could be size-tuned to meet precise device specifications in such proposed applications as high-speed switching devices, high-efficiency lasers, improved memory devices, high-efficiency photocatalytic systems, and light-emitting diodes.[10−12] Interest in group II−VI materials, such as CdS and CdSe, stems from their ability to absorb and emit light in the visible part of the spectrum. However, quantum confinement effects become apparent only in CdS and CdSe particles smaller than 100 Å. Solid-state technologies, such as metalloorganic chemical vapor deposition (MOCVD) and reactive ion etching (RIE), cannot produce such dimensions due to the resolution limitations of current lithographic technology. Alternatively, solution-phase synthesis offers a proven route for production of size-quantized nanoparticles, yet this approach is complicated by high particle surface energies, which necessitate strategies for size stabilization to prevent fusion and to maintain tight nanocrystal size distributions in the quantum-confinement regime.

Two general strategies have been employed for solution-phase group II−VI nanocrystal synthesis: (1) arrested precipitation,[13,14] and (2) reaction compartmentalization. A wide variety of media has been employed to achieve reaction compartmentalization, including polymer gels,[8,15] glasses,[8] ferritins,[16] zeolites,[6] inverse

* To whom correspondence should be addressed.
[†] University of California, Los Angeles.
[‡] University of California, Santa Barbara.
[§] Phone: 310-825-8946. Fax: 310-206-4107. E-mail: harold@seas.ucla.edu.
[||] Phone: (805) 893−4769. E-mail: gorilla@engineering.ucsb.edu.

(1) Fendler, J. H. *Chem. Rev.* **1987**, *87*, 877−899.
(2) Mann, S. *Nature* **1993**, *365*, 499−505.
(3) Blakemore, R. P. *Science* **1975**, *190*, 377−379.
(4) Mann, S.; Archibald, D. D.; Didymus, J. M.; Douglas, T. *Science* **1993**, *261*, 1286−1292.
(5) Steigerwald, M. L.; Brus, L. E. *Annu. Rev. Mater. Sci.* **1988**, *19*, 471.
(6) Stucky, G. D.; MacDougall, J. E. *Science* **1988**, *247*, 669.
(7) Henglein, A. *Top. Curr. Chem.* **1988**, *143*, 113−180.
(8) Wang, Y.; Herron, N. *J. Phys. Chem.* **1991**, *95*, 525−531.
(9) Alivastos, A. P. *Science* **1996**, *271*, 933−937.
(10) Reed, M. *Sci. Am.* **1993**, *268*, 118.
(11) Hagfeldt, A.; Grätzel, M. *Chem. Rev.* **1995**, *95*, 49−68.
(12) Colvin, V. L.; Schlamp, M. C.; Alivastos, A. P. *Nature* **1994**, *370*, 354.
(13) Murray, C. B.; Norris, D.; Bawendi, M. G. *J. Am. Chem. Soc.* **1993**, *115*, 8706.
(14) Vossmeyer, T. *J. Phys. Chem.* **1994**, *98*, 7665−7673.
(15) Lin, J.; Cates, E.; Bianconi, P. A. *J. Am. Chem. Soc.* **1994**, *116*, 4738.
(16) Meldrum, F. C.; Heywood, B. R.; Mann, S. *Science* **1992**, *257*, 522−523.
(17) Mann, S.; Hannington, J. P.; Williams, R. *Nature* **1986**, *324*, 565−567.

S0897-4756(97)00744-8 CCC: $15.00
Published on Web 07/11/1998

micelles,[5] and surfactant vesicles.[2,17] Surfactant vesicles differ from surfactant inverse micelles in that the micelles are used in stabilizing water-in-oil emulsions, while vesicle systems sequester an inner aqueous solution containing reagents from an exterior aqueous solution. Furthermore, micellar systems only partially control reaction compartmentalization due to rapid exchange of micelle contents with one another, and such compartments can increase or decrease in size according to solution conditions. The synthesis of many nanocrystalline materials has been attempted using surfactant vesicle reaction compartments, thereby illustrating[1,18−21] the potential versatility of the method. However, particle sizes were not predictable and size distributions were broad. Use of surfactant vesicles as reaction compartments for nanoparticle synthesis hinges on their ability to contain a prescribed mix of ions or polar species in specified amount from which a particle of controlled size and chemistry can be formed. Most prior work was conducted with vesicles formed by sonication of lipid dispersions, which produces vesicles with relatively broad size distributions and partially hydrolyzed lipid headgroups that are leaky to encapsulated species. Recently, we have shown that a gentle vesicle formation technique, detergent depletion,[22] yields vesicles virtually impermeable to Cd^{2+} and nearly uniform in size—a requirement for intravesicular precipitation of monodisperse CdS particles of controlled dimension.[23,24]

Experimental Section

Monodisperse egg lecithin (phosphatidylcholine) vesicles were produced by detergent depletion using the nonionic detergent *n*-hexyl β-D-glucopyranoside.[24] By controlling the concentration of $CdCl_2$ in solution, the vesicles were made to encapsulate a known number of Cd^{2+} ions, N_{Cd}, from which the CdS nanoparticles are synthesized. Prior to intravesicular particle formation, Cd^{2+} ions external to the vesicles were removed by passing the vesicle dispersion through a cation exchange column (Amberlite IR-120). Immediately after desalting, ammonium sulfide (final concentration of 10 w/v%) was added to the stirred vesicle dispersion, and the mixture was subsequently incubated at room temperature for 8−12 h. Following nanocrystal synthesis, the solution was passed through an anion exchange column (Amberlite IRA-400) to remove all unreacted sulfide. Absorbance measurements were made immediately after particle formation.[24,25]

The particle size can be predicted using a mass balance calculation based on the vesicle diameter, which was determined by the dialysis conditions and confirmed by static light scattering,[26] and the initial encapsulated Cd^{2+} concentration. Assuming complete reaction to form one particle per vesicle, the calculated particle diameter, $d_{p,calc}$, is related to the lattice constant for cubic CdS, a_{CdS} (5.83 Å), and the number of encapsulated Cd atoms per vesicle, N_{Cd}:[24,27]

$$d_{p,calc} = a_{CdS}\left[\frac{3N_{Cd}}{2\pi}\right]^{1/3} \quad (1)$$

For a sufficiently narrow vesicle size distribution and only one crystal forming per vesicle, the calculated particle diameter should match the measured diameter if growth is compartmentalized.

Cryo-transmission electron microscopy (cryo-TEM) clearly shows that only one CdS nanoparticle of controlled size precipitates within each vesicle; in addition, there is a specific orientation of the crystal with the vesicle bilayer. Aqueous specimens were vitrified by plunging thin (<0.2 μm) sample films supported on polymer-coated electron microscope grids into liquid propane cooled by liquid nitrogen.[28−30] The frozen samples were imaged at ≤−160 °C in a JEOL 100CX TEM operating at 100 kV using a Gatan low temperature sample stage and transfer system. Contrast in the image was produced primarily by phase contrast, which requires the objective lens to be underfocused to enhance phase shift between the microstructure of the system and the vitrified water.[31] To minimize radiation damage from the electron beam, an area adjacent to the final image was used to optimize defocus before recording the micrograph from a nearby area.[32]

Results and Discussion

Figure 1 shows a series of cryo-TEM images of CdS nanocrystals grown within lecithin vesicles. Cryo-TEM enables visualization of the vesicle wall and the particle in situ as projections onto the image plane of the micrograph. Figure 1A is an image of vesicles containing Cd^{2+} ions before desalting and prior to CdS particle formation. The vesicle wall generates sufficient phase contrast in areas where the lipid bilayer is parallel to the electron beam direction (perpendicular to the sample plane), giving rise to a single gray, circular ring. Figure 1B shows the same preparation after desalting and the addition of ammonium sulfide, which produced barely visible CdS nanocrystals of $d_{p,calc} \sim 30$ Å in size. These represent the smallest CdS particles that we could resolve using this technique. By adjusting the concentration of Cd^{2+} in the vesicles, we could control the final size of the CdS nanocrystal formed. Figure 1C shows a sample in which $d_{p,calc} \sim 38$ Å CdS nanocrystals were

(18) Mann, S.; Hannington, J. P. *J. Colloid Interface Sci.* **1988**, *122*, 326−335.
(19) Heywood, B. R.; Fendler, J. H.; Mann, S. *J. Colloid Interface Sci.* **1990**, *138*, 295−298.
(20) Bhandarkar, S.; Bose, A. *J. Colloid Interface Sci.* **1990**, *135*, 531−538.
(21) Yaacob, I. I.; Bhandarkar, S.; Bose, A. *J. Mater. Res.* **1993**, *8*, 573−577.
(22) Kagawa, Y.; Racker, E. *J. Biol. Chem.* **1971**, *246*, 5477.
(23) van Zanten, J. H.; Monbouquette, H. G. *Biotechnol. Prog.* **1992**, *8*, 546.
(24) Korgel, B. A.; Monbouquette, H. G. *J. Phys. Chem.* **1996**, *100*, 346−351.
(25) Interference of vesicle light scattering on particle absorbance measurements is eliminated by collapsing vesicle compartments with the nonionic detergent octyl β-D-glucopyranoside (OG), prior to scanning.
(26) van Zanten, J. H.; Monbouquette, H. G. *J. Colloid Interface Sci.* **1991**, *146*, 330.
(27) Raleigh−Gans−Debye theory and multiangle static light scattering measurements of vesicles before particle formation are used to determine the vesicle outer diameter which, coupled with the bilayer thickness (3.7 nm) and the encapsulated Cd^{2+} concentration, gives N_{Cd}.
(28) Thin aqueous specimens were prepared on 300 mesh, lacey carbon substrate, copper TEM grids (Ted Pella, Redding, CA) inside a temperature- and humidity-controlled environmental chamber at 25 °C. All vesicle solutions were diluted with MilliQ water, to a lipid concentration of approximately 1 mg/mL for specimen preparation. A thin film of liquid was produced by blotting a sample droplet with Whatman chemical-grade filter paper. The specimens were vitrified by plunging into a liquid propane−ethane mixture cooled to −180 °C. Vitrified specimens were transferred under liquid nitrogen to a Gatan Model 626 Cryotransfer System (Gatan, Inc., Warrendale, PA) and were inserted into the microscope for imaging at −165 °C.
(29) Bellare, J. R.; Davis, H. T.; Scriven, L. E.; Talmon, Y. *J. Electron Microsc. Technol.* **1988**, *10*, 87−111.
(30) Dubochet, J.; Adrian, M.; Chang, J. J.; Homo, J. C.; Lepault, J.; McDowall, A. W.; Schultz, P. *Q. Rev. Biophys.* **1988**, *21*, 129−228.
(31) Fryer, J. R. *The Chemical Application of Transmission Electron Microscopy*; Academic Press Inc.: New York, 1979.
(32) Images are recorded on Kodak SO163 Electron Imaging Film and developed in a 1:1 Kodak D19 solution for 12 min. The micrograph negatives are scanned electronically with an AGFA Arcus II scanner at 400 dpi and receive minimal contrast adjustment using Adobe Photoshop. All features recognized in the scanned images are distinguished easily in the original micrographs.

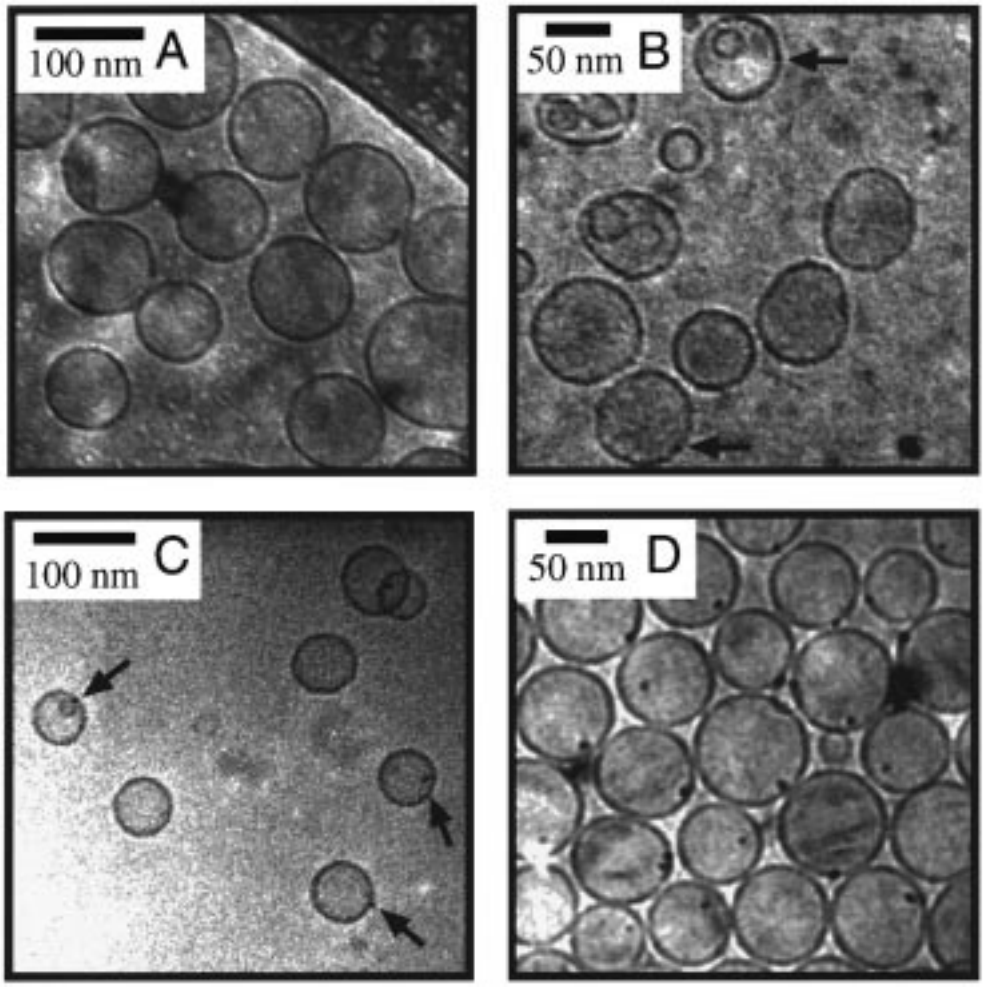

Figure 1. Cryo-TEM images of egg phosphatidylcholine vesicles. (A) Vesicles prior to desalting of unencapsulated Cd^{2+}. (B) 30 Å CdS nanocrystals (arrows) are barely visible as small black spots associated with the vesicle membrane. (C) 38 Å CdS nanocrystals (arrows) appear larger and more frequently, as the particle size approaches the width of the vesicle bilayer. (D) 59 Å CdS nanocrystals are clearly visible and appear both inside and around the ring of the vesicle bilayer. In nearly all cases, only one particle per vesicle is produced, and the image suggests that the particles are associated closely with the membrane bilayer.

produced. The nanocrystals appear larger than in the 30 Å sample and are now comparable in size to the width of a bilayer. Figure 1D shows a large assembly of vesicles that contain single CdS nanocrystals at a higher Cd^{2+} concentration. Most vesicles contain only a single nanocrystal of approximately two bilayer thicknesses, as expected given that $d_{p,calc} \sim 59$ Å. The cryo-TEM pictures of Figure 1 provide strong evidence that only one particle forms per vesicle and the particle size decreases with decreasing N_{Cd}, as expected from mass balance calculations. These results, taken in conjunction with earlier high-resolution TEM measurements of particle sizes and size distributions, confirm that true reaction compartmentalization is achieved with this system.[24]

Figure 2 shows the room-temperature UV−visible absorbance spectra for six different CdS preparations within vesicles. The spectra display the usual size-dependent features of size-quantized CdS nanocrystals. As expected, the absorption edge (which for a bulk crystal corresponds to the band gap energy) shifts to shorter wavelengths with decreased particle size due to quantum confinement of electrons. An exciton peak resulting from discretization of the HOMO → LUMO (highest occupied molecular orbital → lowest unoccupied molecular orbital) electronic transition also appears in the spectra. This peak increases in prominence and shifts to higher energy with decreased size, which is indicative of relatively narrow nanocrystal size distributions and tight size control. As the particle size is decreased below ~25 Å in diameter, discrete higher energy transitions become discernible, which generally are not observed in preparations with broad size distributions. Finally, the exciton energies for the calculated particle diameters correspond well with those expected from theory and with other data found in the literature.[24]

The vast majority of CdS particles in Figure 1 that are dark and in focus with the vesicle wall appear to be adsorbed to or embedded in the vesicle wall. Nanocrystals that appear inside the vesicle and away from the gray ring of the vesicle wall are also likely associated with sections of the vesicle bilayer, but are not as apparent from the cryo-TEM images. The proximity of the particles to the vesicle wall suggests a process of membrane-mediated nucleation and growth of the nanocrystals. This suggestion is confirmed by Figure 3A,B, which shows high magnification images of several nanocrystals from the 59 Å specimen in which the contrast of the images has been adjusted to produce

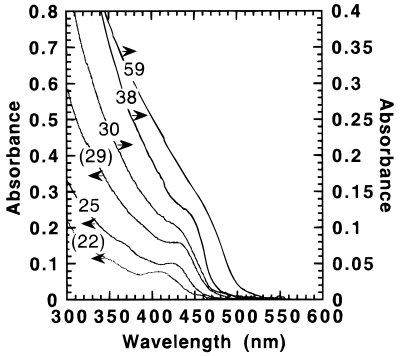

Figure 2. Room-temperature optical absorbance spectra for CdS nanocrystals grown within egg phosphatidylcholine vesicles. The particle diameters (in Å) in parentheses were determined from high-resolution TEM images; $d_{p,calc}$ for these samples were 19.7 and 27.6 Å. All other particle diameters reported are calculated particle diameters. The top three curves correspond to the samples examined with cryo-TEM in Figure 1. The vesicle sizes and initial encapsulated Cd^{2+} concentrations for the 30, 38, and 59 Å particles were 60, 60, and 73 nm and 6.3, 11.4, and 25 mM, respectively.

faint vesicle walls and bold crystals. The images clearly show the crystals to be nonspherical, in agreement with our earlier high-resolution TEM images which indicated a ratio of long to short axis of about 1.2.[24] In both figures, the longer dimension axis of the nanocrystal appears to be tangentially aligned with the vesicle membrane. Other images (not shown) showed the same preferential alignment. Figure 3C, an image of a crystal not associated with any vesicle membrane and of different orientation with respect to the image plane, indicates the contrast-resolved features are not artifacts generated by the lipid bilayer itself, microscope drift, or the scanning process. The nanocrystal in Figure 3C was likely ejected from a lysed vesicle during cryo-TEM specimen preparation. Figure 3D is a high-resolution TEM image of a ~55 Å diameter CdS nanocrystal (outlined) oriented to display the spacing of the {220} lattice plane for cubic CdS.[24] The specimen was produced by allowing nanocrystal sample to dry directly onto a carbon-coated TEM grid. The image clearly shows the high degree of crystallinity for the particles formed inside vesicles.

The anisotropy and orientation of the nanocrystals is somewhat consistent with the observed anisotropy of CdS nanocrystals grown under Langmuir monolayers of stearic acid (SA).[33] These experiments revealed a preferred direction of growth of rodlike CdS nanocrystals corresponding to templating between the {220} lattice plane of cubic CdS and the $(10\bar{1}0)$ plane of the hexagonal close-packed SA monolayer. However, isotherms of egg PC monolayers over a $CdCl_2$ subphase (not shown) do not provide any evidence of a condensed phase existing in our system. Therefore, it is unlikely that the observed anisotropy and orientation of CdS grown inside egg PC vesicles is generated through a specific epitaxial relationship, rather, the vesicle membrane orients the growth of the nanocrystal and somehow enhances the nucleation. Other lipid systems do form ordered condensed phase vesicles, and may prove capable of providing oriented growth of nanocrystals inside vesicles.

(33) Pan, Z. Y.; Shen, G. J.; Zhang, L. G.; Lu, Z. H.; Liu, J. Z. *J. Mater. Chem.* **1997**, *7*, 531−535.

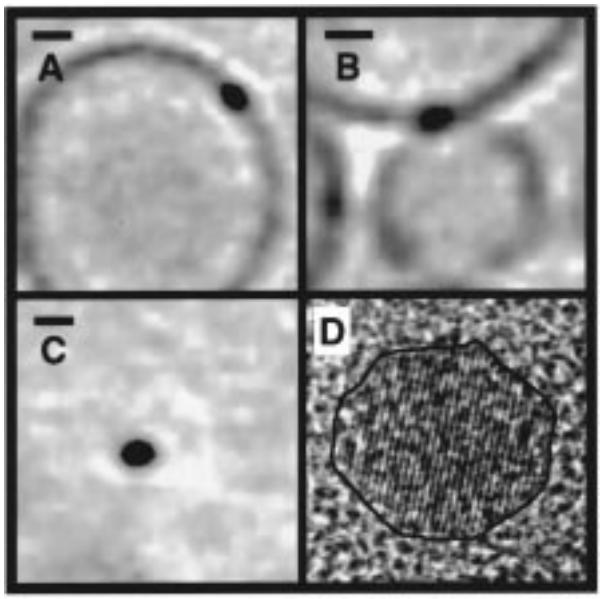

Figure 3. High-magnification images of nanocrystals formed inside unilamellar vesicles. (A, B) Cryo-TEM of 59 Å CdS inside vesicles show that the crystals associate with the membrane bilayer and that the long axis of the crystal orients parallel to the bilayer surface. Images have been contrast-enhanced. (C) The nonspherical shape of the nanocrystals is evident in crystals that have been ejected from vesicles during cryo-TEM specimen preparation. Scale bars are 100 Å. (D) TEM image (not cryo-TEM) of an approximately 55 Å diameter CdS nanocrystal (outlined) resting on the {110} plane and displaying the spacing between the {220} planes.

Conclusions

In conclusion, we have demonstrated compartmentalized growth of single quantum-sized CdS nanocrystals within egg phosphatidylcholine vesicles formed by detergent depletion. Cryo-TEM and particle absorbance measurements confirm the particle size to be predictable on the basis of the vesicle diameter and the encapsulated Cd^{2+} concentration. The cryo-TEM images show a likely association between the vesicle bilayer and the CdS particles that could aid in understanding nonepitaxial, membrane-mediated crystal growth. This approach to the synthesis of nanocrystalline materials may prove useful for exploration of a wide variety of nanoparticulate materials not conveniently accessible by other means, including doped semiconductor quantum dots of specified stoichiometry.

Acknowledgment. B.A.K. is grateful for a U.S. Department of Education Pollution Prevention Fellowship (Award# P200A40732). M.T.K. and J.A.Z. are thankful for support under NSF Grant CTS-9319447.

CM970744K